Mechanisms of Equinatoxin II-Induced Transport through the Membrane of a Giant Phospholipid Vesicle

M. Mally,* J. Majhenc,* S. Svetina,*† and B. Žekš*†

*Institute of Biophysics, Faculty of Medicine, University of Ljubljana, 1000 Ljubljana, Slovenia; †J. Stefan Institute, Jamova 39, 1000 Ljubljana, Slovenia

ABSTRACT Protein equinatoxin II from sea anemone *Actinia equina* L. was used to form pores in phospholipid membranes. We studied the effect of these pores on the net transmembrane transport of sucrose and glucose by observing single giant (cell-size) vesicles under the phase contrast microscope. Sugar composition in the vesicle was determined by measuring the width of the halo, which appears around the vesicle in the phase contrast image. The transport of sugars was induced when a vesicle, filled with the sucrose solution, was transferred into the isomolar environment of a glucose solution with added equinatoxin II. Typically, a vesicle grew to a critical size, then the membrane broke by bursting and the vesicle shrank, started to grow again, and the whole process was repeated. The consecutive membrane breaks occurred in the same spot. The observed behavior was interpreted by the diffusion flow of the glucose molecules through the equinatoxin II-induced pores and the consequent increase of the vesicle water content. The burst relaxed the critically strained membrane, which then apparently resealed. A mathematical model of the described behavior was developed and was used to obtain the equinatoxin II-induced membrane permeability for the glucose molecules. Its dependence on the equinatoxin II concentration is in agreement with the previous reports.

INTRODUCTION

Actinoporins are pore-forming proteins with potential applications in pharmacology and biotechnology (Avila et al., 1989; Bhakdi et al., 1993; Russo et al., 1997). They are also used as tools for investigating the permeabilization of membranes and the transmembrane transport of solutes (Belmonte et al., 1993; Tejuca et al., 1996; De Los Rios et al., 1998). Their mode of action (Maček et al., 1994; Zorec et al., 1990), their structure (Belmonte et al., 1994; Athanasiadis et al., 2001), their interaction with the membranes (Maček et al., 1995; Caaveiro et al., 2001), and the mechanism of the pore-formation (Belmonte et al., 1993; Athanasiadis et al., 2001) are well documented.

Actinia equina L. is a widespread sea anemone that produces many toxic proteins. One of the isolated proteins is actinoporin equinatoxin II (EqT-II) with molecular mass of 19.5 kDa. It is a basic protein with a single polypeptide chain and acts on cellular and model lipid membranes. Its cardiotoxic (Ho et al., 1987; Lee, 1989), hemolytic (Maček and Lebez, 1981), cytolytic, and cytotoxic (Batista et al., 1990) effects have been reported. Although the mechanism of its action is not yet completely understood, it is known to be a very potent toxin that increases the permeability of membranes for small ions and solutes by forming discrete pores. The functional radius of a pore has been estimated to be ~1 nm (Belmonte et al., 1993). It was suggested that the pore is in fact an oligomeric channel comprising an average of three to four EqT-II monomers. The toxin binds preferentially to membranes that are composed of lipid mixtures (Caaveiro et al., 2001; Valcarel et al., 2001). It was observed that the toxin does not act on the membranes comprised of pure phosphatidylcholine but causes leakage from the vesicles when sphingomyelin is also present in the membrane (Belmonte et al., 1993).

Previous studies of membrane permeabilization and of transport through the toxin-induced pores have all been performed on suspensions of submicron unilamellar vesicles, loaded with the fluorescent marker calcein (Belmonte et al., 1993; Tejuca et al., 1996; De Los Rios et al., 1998). The release of calcein from the vesicles after the introduction of the toxin showed that the vesicle membranes become permeable for small molecules and ions. The rate and the extent of permeabilization can be calculated. However, these studies do not reveal the actual mechanism of releasing the vesicle content. An open issue remains whether the introduction of the toxin causes the vesicles to lyse or whether they persist and release their content continuously through the toxin induced pores. In the latter case, do they release all or just a part of their contents? To resolve this and to contribute to an understanding of the mechanism of the solute transport and the dynamics of the solute release, a new methodology to observe and analyze the behavior of single giant vesicles (with radii ~50 μm) was introduced.

In a typical experiment the vesicles were prepared loaded with sucrose solution. Using a micropipette, a vesicle was brought from the original solution into a glucose solution containing EqT-II, which incorporated into the membrane and formed pores. Due to the transport of sugar molecules through the EqT-II-induced pores, the composition of the sugar mixture inside the vesicle was changing with time. Phase-contrast microscopy was used to observe the vesicle

Submitted July 27, 2001, and accepted for publication April 24, 2002.

Address reprint requests to Dr. Mojca Mally, University of Ljubljana, Institute of Biophysics, Faculty of Medicine, Lipiceva 2, SL-1000 Ljubljana, Slovenia. Tel.: 386-1-543-7600; Fax: 386-1-431-5127; E-mail: mojca.mally@biofiz.mf.uni-lj.si.

0006-3495/02/08/944/10 $2.00

continuously and to avoid bleaching problems with fluorescent markers. The sugar composition of the vesicle contents was determined from the feature of the phase - microscopy image that a halo occurs around the vesicle cross-section as the consequence of the difference between the refraction indices of the inner and the outer sugar solutions. We were able to follow the changes in composition of the vesicle contents by measuring the width of the vesicle halo. From experimental data and by applying a theoretical analysis describing the transport of the sugar molecules, accompanied by water, into the vesicle, we determined the critical radius. At a critical radius, the vesicle bursts, and the strained vesicle membrane is relaxed by the ejection of the internal solution.

In the next section our experimental procedure is described. In the Results section we present the observations and a theoretical analysis of the system behavior, by which it is possible to obtain the permeability of the membrane at different concentrations of EqT-II. In the Discussion section we compare the observations and measurements with the predictions of the analysis and with the conclusions of other studies.

MATERIALS AND METHODS

Materials

Vesicle membranes were made from phosphatidylcholine (1–palmitoyl–2–oleoyl–*sn*–glycero–3-phosphocholine (POPC) (Avanti Polar Lipids Inc., Alabaster, AL)) and 10% or 20% of sphingomyelin (SM) from bovine brain, (Sigma, St. Louis, MO). Both lipids were available in powder form and were dissolved in a mixture of 2:1 (v/v) chloroform-methanol to 1 mg/mL. The solution was stored at −15°C.

Anhydrous, pro analysis (p.a.) glucose with molar weight M = 180.16 g/mol and p.a. sucrose with molar weight M = 242.3 g/mol (Kemika, Zagreb, Croatia) were used without prior purification.

Equinatoxin II was purified to homogeneity from the sea anemone *Actinia equina* L. in the laboratory of Department of Biology, Biotechnical Faculty, University of Ljubljana, Slovenia. The toxin was stored in water at a concentration 0.2 mg/mL at −4°C.

Preparation of the vesicles

Phospholipid vesicles were prepared by electroformation by a slightly modified method of Angelova (Angelova et al., 1992). First, a desired mixture of 12 μL of the solution of POPC and SM in chloroform-methanol was placed on each of the two platinum electrodes under low pressure for 2 h so that the solvent evaporated. The electrodes were then inserted into a cell for the electro-formation process and fixed in parallel 0.5 cm apart. The cell was filled with 2 mL of the sugar solution (usually sucrose), required in the vesicles, and sealed. Alternating current of frequency 10 Hz and 5 V amplitude was applied across the electrodes. After 2 h, when the vesicles had grown enough, the frequency was reduced to 5 Hz and the voltage amplitude to 4 V. After 15 min, frequency and amplitude were decreased again to 2.5 Hz and 3 V, respectively, and after a further 15 min, finally to 1 Hz and 2 V. These conditions were maintained for at least 30 min more to allow the vesicles to detach from the electrodes. Vesicles prepared by this method are in general spherical, unilamellar, and most of them have no visible protuberances. The sugar solution with vesicles can be stored in a closed plastic beaker and used for a few days.

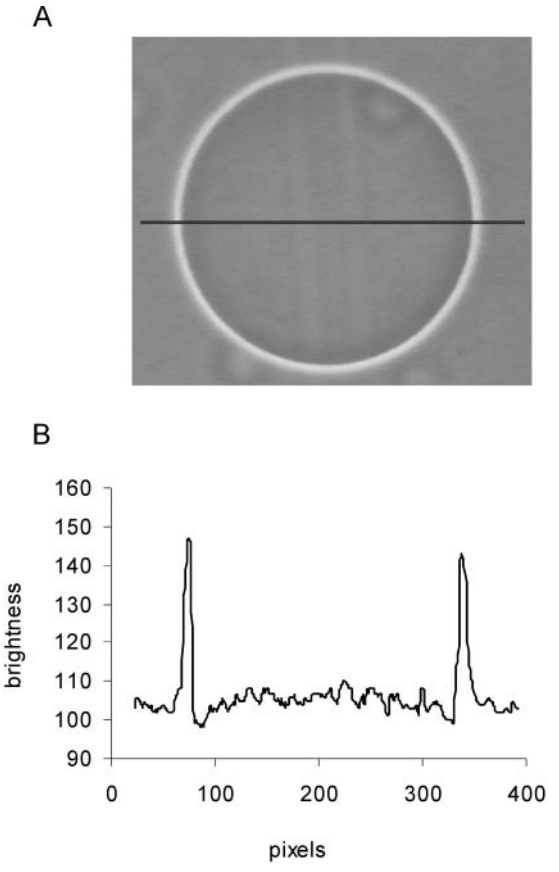

FIGURE 1 Halo around the object in the phase-contrast image. (*A*) Halo appears around the vesicle because the refraction index of the vesicle contents (sucrose solution) is different from the refraction index of the surroundings (isomolar glucose solution). (*B*) Measurement of the brightness on the vesicle cross-section along the indicated line. The halo width is defined as the width of the peak at the half height.

Methods

The vesicles were observed under an inverted optical microscope (Opton IM35, Zeiss) with phase-contrast objective (40×, NA 0.60, Zeiss), and condenser (Phako IV Z7, Zeiss). The experiment was monitored on the screen, using a high resolution camera (CCD-IRIS, Sony). The observations were recorded on S-VHS-XP pro, TDK tapes. For analysis the images were digitized by a Data Translation frame grabber (DT 2851); in the transformed image of 512 × 512 pixels, each pixel represented an area of 0.4 × 0.28 μm^2 and its brightness corresponded to the brightness level from 0 to 255.

If observed in the environment of a glucose solution, the vesicles containing sucrose solution appear dark (as at the same concentration the refraction index of the sucrose solution is higher than that of the glucose solution) against the background. A white halo, characteristic of a phase-contrast image, appears around the vesicle (Fig. 1 *A*). Transparent biological objects modify only the phase of the light passing through them as their refraction indices differ from that of their surroundings. The amplitude of the light remains the same and thus the objects remain invisible if observed under the bright field microscope. In phase-contrast microscopy, the image of the object is obtained by transforming phase differences into amplitude differences by a phase plate. In the process of image formation, a part of the first diffraction maximum is lost, and on the boundary between the observed object and

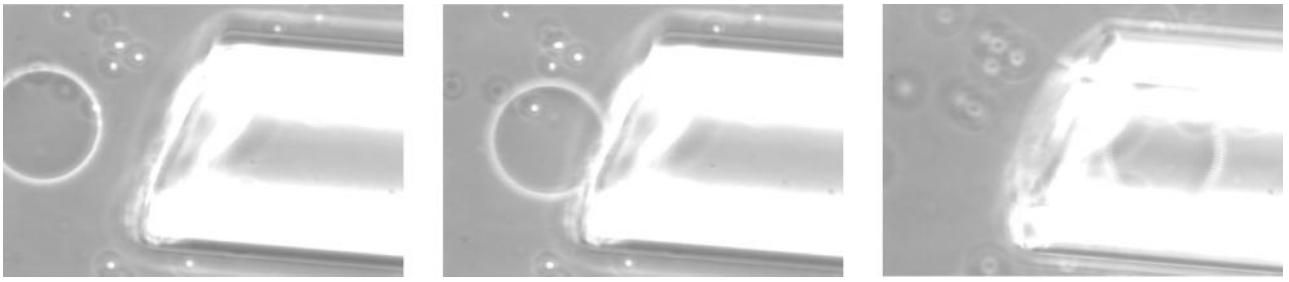

FIGURE 2 Aspiration of the vesicle into a micropipette. Micropipettes had an inner diameter of ~160 μm.

its surroundings with a different refraction index a contrast rim, a halo occurs, detected as a brightness peak on the densiometric graph (Fig. 1 *B*). The width of the halo depends on the difference of the refraction indices of the object and its surroundings, the size of the observed object, and on the properties of the microscope (Pluta, 1989). In our experiment, the halo width was defined as the width of the peaks at half height when measuring the brightness of the pixels along the indicated line on the image cross-section (Fig. 1).

Experimental procedure

The measurement cell has two separate compartments. The first was filled with a mixture of vesicle suspension and isomolar glucose solution. The vesicles sank to the bottom of the cell. Vesicles were taken one at a time, the criteria being that they had no visible protuberances, were unilamellar and had an appropriate size (see below). Vesicles were transferred using a micropipette filled with glucose solution with a radius a little bigger than the radii of the vesicles that we wanted to transfer. We aspirated the vesicle into the micropipette (Fig. 2) and transferred it into the other compartment of the measurement cell.

To determine the relations between halo width and vesicle size and between halo width and the composition of the vesicle contents, a number of vesicles were analyzed. The halo width increases with increasing radii of the vesicles but is constant for radii larger than 40 microns (Fig. 3). By choosing vesicles with radii ~50 μm the influence of vesicle size on halo width was excluded. To explore the dependence of halo width on the composition of the vesicle contents, we prepared vesicles that contained solutions with different fractions of sucrose and glucose. The width of the halo as a function of the sucrose fraction inside the vesicle was determined for total sugar concentrations of 0.5 and 0.2 M (Fig. 4). The calibration curves are approximately linear. If extrapolated to the point, where the solution inside the vesicle is the same as the solution outside the vesicle (0% of sucrose inside the vesicle), the halo width is still different from zero, which can be attributed to the refraction index of the membrane itself. The measured absolute halo width is larger when larger total sugar concentration is used.

In a typical experiment the vesicles, containing sucrose solution, were transferred at zero time into the isomolar glucose solution with EqT-II. We followed the narrowing of the vesicle halo and thus the decreasing of the sucrose fraction inside the vesicle. When analyzing images we were measuring the diameter of the vesicle and the width of the halo around the vesicle. The experiments were carried out at room temperature.

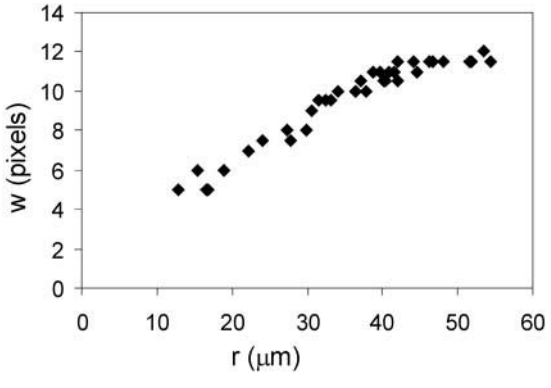

FIGURE 3 Dependence of the halo width (w, in pixels) on the vesicle size (r).

RESULTS

Modifications of the vesicle after the application of equinatoxin II

Equinatoxin II has some clearly visible effects on phospholipid vesicles. A few minutes after a sucrose-containing vesicle is transferred into the glucose solution with added EqT-II, the vesicle starts to grow. When it attains a certain size, the vesicle bursts, ejecting a part of its contents, visible as a dark cloud on a brighter background (Fig. 5), and shrinks back to its initial size. The vesicle starts to swell again, and the whole process is repeated, the time between the successive bursts increasing (Fig. 6). The bursts appear to occur always on the same spot in the membrane. The process of swelling and bursting stops when the halo almost disappears and the vesicle interior is as bright as the surroundings (Fig. 7 *A*).

Vesicles, used the same day as they were prepared behaved differently in that after the bursts they shrunk to smaller and smaller sizes (Fig. 7 *B*). Such a diminishing of the vesicle size indicates a loss of membrane during the bursts. However, it could be seen that the membrane forms cylindrical and spherical protuberances inside the vesicle. In further experiments the equilibrated, 1- to 5-day-old vesicles, which did not show this behavior, were used.

In the control experiment, we transferred the vesicles into a pure glucose solution (containing no equinatoxin II). We detected no changes of the vesicles in typical observation times and we concluded that phospholipid membranes are virtually impermeable to the sucrose and glucose.

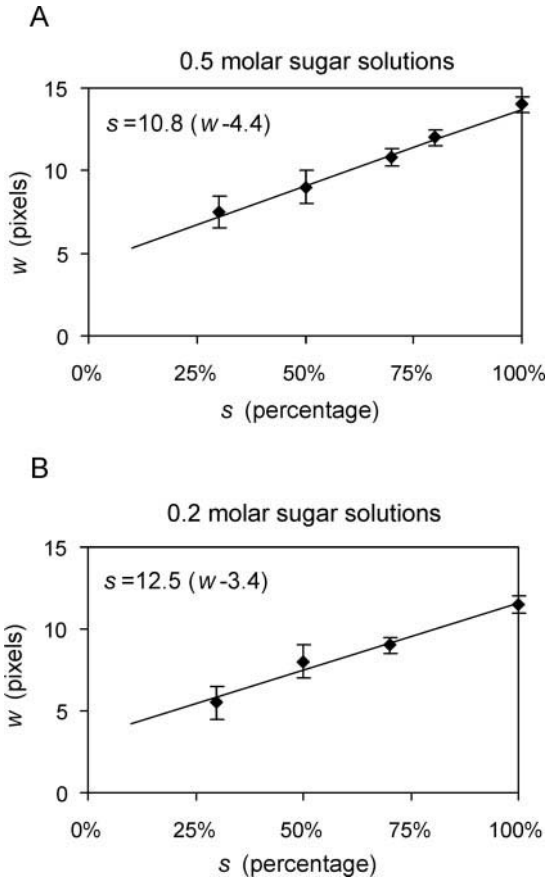

FIGURE 4 The width (w, in pixels) of the halo around the vesicle as a function of the fraction of sucrose solution (s, in percentage) inside the vesicle. The vesicles contain either (A) a 0.5 M mixture of glucose and sucrose solution and are surrounded with isomolar glucose solution or (B) a 0.2 M mixture of glucose and sucrose solution and are surrounded with isomolar glucose solution. The radii of the chosen vesicles in the experiment are ~50 μm.

Observations and related conclusions

The experiment was carried out and the vesicles observed under the following varied parameters: 1) the concentration of the toxin; 2) the total concentration of sugar solutions (0.2 or 0.5 M sugar solutions were used); and 3) the composition of the membrane (we used lipid compositions with 10% or 20% of SM).

The concentration of toxin in the glucose solution, into which the vesicle was transferred, influenced the speed of the process. The process of swelling and bursting and narrowing of the halo was faster when the toxin concentration was larger (compare Fig. 8, A and B). There was no significant difference between the behavior of the vesicles with different molarities of sugars (compare Fig. 8, B and C). The vesicles with larger fraction (20%) of SM in the membrane went through the same process as the vesicles with only 10% of SM in the membrane, only faster (compare Fig. 8, C and D).

From the observations we concluded that originally impermeable membranes became permeable; the permeability was larger when the toxin concentration was larger and when the fraction of SM in the membrane was larger, which is consistent with previous experiments on samples of submicron vesicles (Belmonte et al., 1993). The bursting of the membrane did not result in lysis of the vesicle but allowed relaxation of the membrane tension by ejection of the inner solution.

An "inverted" experiment was carried out where the vesicles filled with glucose were transferred into the isomolar sucrose solution. These vesicles floated to the top of the measurement cell. In the sucrose solution a certain amount of EqT-II was added. The observations (not shown) revealed that the vesicles became flaccid. The halo remained practically the same during typical observational times. This indicates that the smaller glucose molecules can diffuse through the EqT-II-induced pores out of the vesicle, whereas the flow of the bigger sucrose molecules into the vesicle is negligible.

Theoretical analysis

The summary of our observations and measurements, together with the previous knowledge about the system serves as a basis of the following theoretical model.

The estimated membrane water permeability $P_w = 3 \times 10^{-3}$ cm/s (Olbrich et al., 2000) gives the characteristic relaxation time of our system (vesicles with radii $r = 50$ μm) $\tau_w = r/3P_w = 0.7$ s; the permeability of intact lipid membranes for glucose molecules is approximately $P_g = 10^{-10}$ cm/s (Jung, 1971), which yields a characteristic relaxation time for glucose $\tau_g = 1.7 \times 10^7$ s = 4629 h. In the

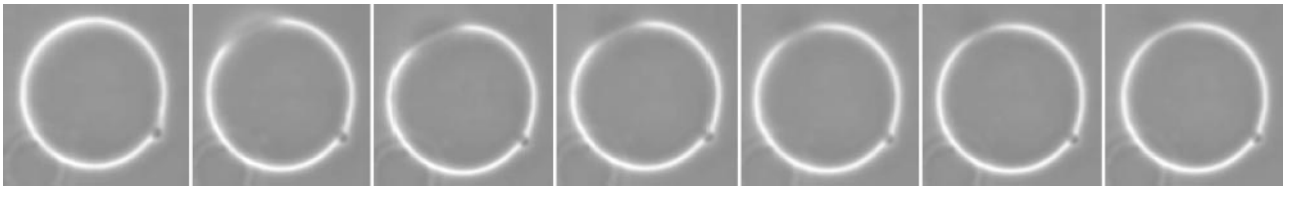

FIGURE 5 Illustration of the vesicle burst. By bursting the vesicle ejects part of its contents, visible as a dark cloud (in upper left corner). In the first and the last frame the intact and the resealed membrane are shown, respectively. Typical bursts last ~0.3 s.

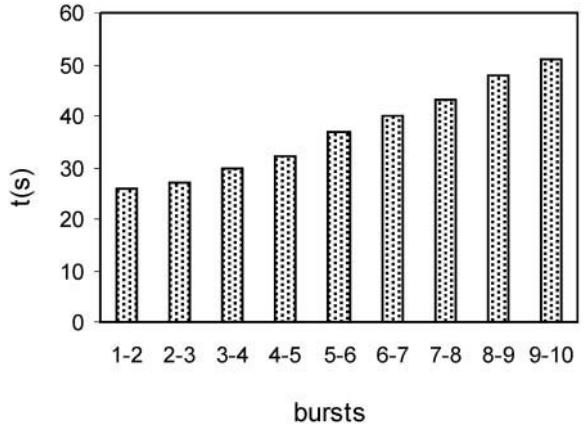

FIGURE 6 Measured time intervals between successive bursts.

control experiments, where no EqT-II was used, no significant changes in sugar concentrations were recorded in observations more than 1 h long. After comparing these characteristic times with a typical time of the experiment, which was approximately 20 min, we assumed that water freely traverses the membrane and can instantly equalize the pressure differences that are caused osmotically and mechanically, whereas the membranes are virtually impermeable for any larger molecules.

EqT-II induces pores in the phospholipid membranes. According to the "inverted" experiment we can conclude that the molecules of glucose can pass through the pores much faster than the molecules of sucrose. This conclusion is supported by the data on the pore radius (Belmonte et al., 1993; Maček et al., 1995), which was estimated to be ~1 nm. We assumed that the glucose molecules (with approximate radii 0.44 nm) diffuse through EqT-II-induced pores, but the membranes are not permeable to the larger sucrose molecules (with radii ~0.56 nm).

In our experiment the vesicle, which contains sucrose solution, is surrounded by the glucose solution. With the membrane that is now permeable to smaller molecules, the glucose molecules from the outer solution diffuse into the vesicle. There is a tendency for the sugar concentration inside the vesicle to increase, but water is driven into the vesicle by the osmotic pressure and the osmotic equilibrium with the outer solution is instantly established. The vesicle therefore grows, but when the critical value of membrane tension is reached, the membrane bursts. The vesicle ejects part of its contents, and its radius decreases back to the value where the membrane is unstrained. The ejected solution was seen as a dark cloud, which indicates that the bulk flow out of the vesicle "pushes" the molecules away from the hole, and the number of glucose molecules that have diffused into the vesicle during the short burst is negligible compared with the number that have been ejected from the vesicle. We can assume that the ratio of sugar concentrations inside the vesicle does not change during the burst.

After the membrane is resealed, the transport of glucose molecules through the pores continues, and the vesicle starts to grow again. The fraction of glucose in the vesicle increases. The glucose diffusion flow, which is proportional to the membrane permeability and the glucose concentration difference, decreases and the time between successive bursts lengthens (Fig. 6). Such behavior can be consistently described by assuming that the permeability of the membrane and the number of pores are constant. As the times before the first burst are different for different vesicles (some vesicles are flaccid and need additional time to become spherical), the first burst is a starting point of the

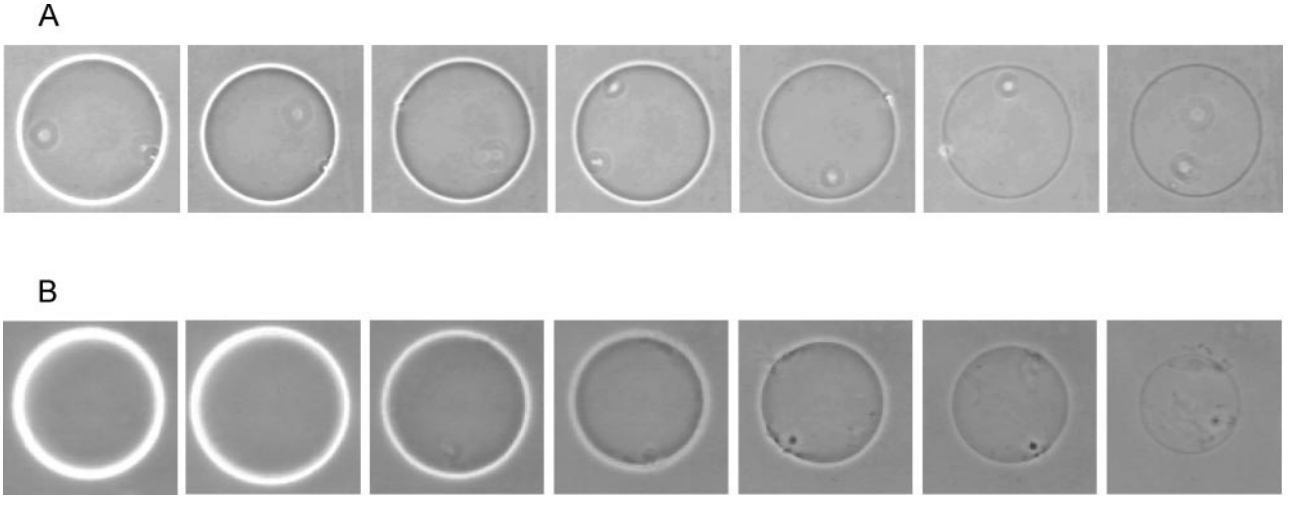

FIGURE 7 Disappearance of the halo and fading of the vesicle in the presence of EqT-II. There is ~5 min between the successive frames. (*A*) Vesicle is 5 days old. (*B*) Freshly prepared vesicles behaved differently in that they were diminishing in size and protuberances were forming on the membrane, whereas the vesicle maintained its spherical shape.

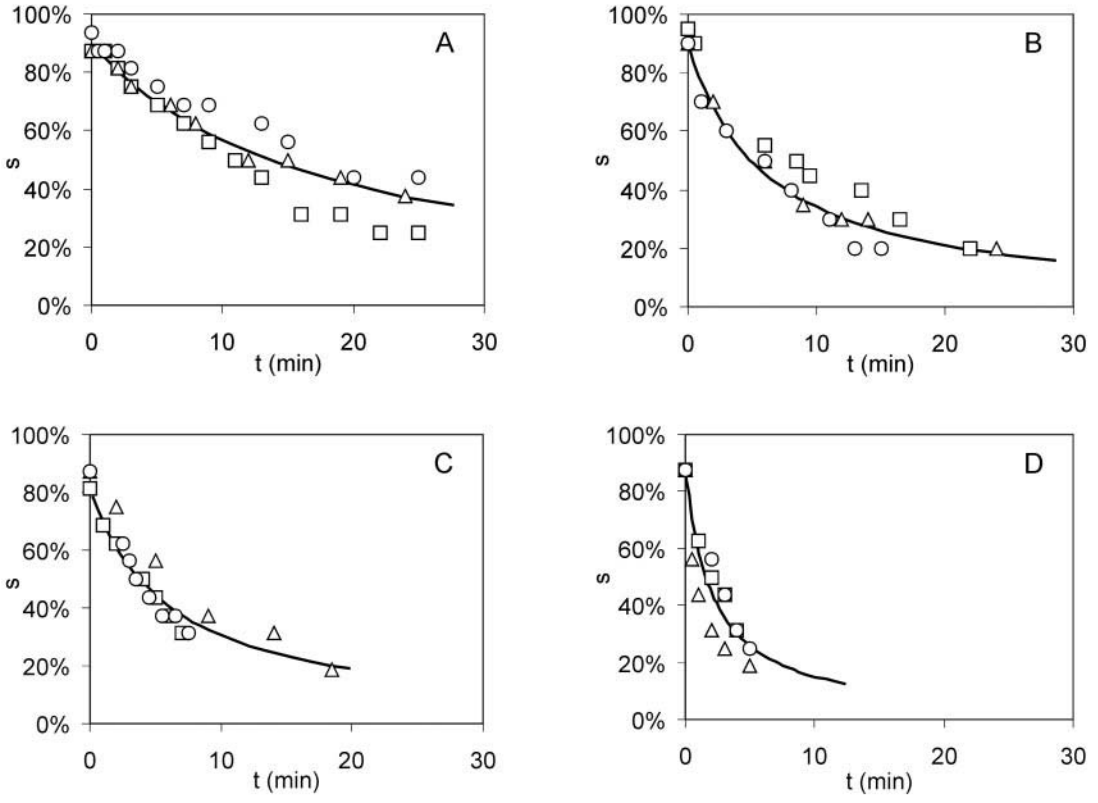

FIGURE 8 Time dependence of the sucrose fraction (s) inside the vesicle. The measurements are illustrated for four groups of vesicles of varied membrane composition, used EqT-II concentration, and molarity of sugar solutions: (A) 90% POPC and 10% SM, 2 μg/mL, 0.5 M; (B) 90% POPC and 10% SM, 4 μg/mL, 0.5 M; (C) 90% POPC and 10% SM, 4 μg/mL, 0.2 M; (D) 80% POPC and 20% SM, 4 μg/mL, 0.2 M; Three of the analyzed vesicles are shown for each group. The full line represents the results of the theoretical analysis of the experiment.

comparison of the experimental data and the predictions of the model.

We can now proceed with the mathematical representation of this model. The osmotic pressure causes the water to flow into the relaxed, spherical vesicle with radius r_0. The vesicle swells, and the membrane is more and more strained. The elastic energy of the membrane with surface $A = 4\pi r^2$ is:

$$W = \frac{1}{2} k_a \frac{(A - A_0)^2}{A_0}, \tag{1}$$

in which k_a is the area expansivity elastic constant and $A_0 = 4\pi r_0^2$ is the vesicle area when the membrane is not strained. The radius of the strained vesicle (r) depends on the difference (p) between the inner and the outer pressures. The requirement for mechanical equilibrium

$$pdV = dW \tag{2}$$

gives the dependence of the pressure difference on the radius of the vesicle:

$$p(r) = \frac{2k_a(r^2 - r_0^2)}{r_0^2 r}. \tag{3}$$

It is assumed that due to fast transport of water through the membrane the osmotic equilibrium is instantly established. In such a quasistatic equilibrium situation the pressure difference equals the osmotic pressure difference, caused by the difference of the sugar concentrations inside (C_g and C_s for glucose and sucrose concentration, respectively) and outside (C_{go}) the vesicle:

$$p(r) = kT(C_g + C_s - C_{go}), \tag{4}$$

where k is Boltzmann constant, T, the temperature, and concentrations are expressed as number densities. We assumed that the concentration of glucose molecules outside the vesicle is constant, the outer volume (the volume of the measurement cell) being much larger than the volume of the vesicle. The number of sucrose molecules (N_s) inside the vesicle remains constant until the vesicle bursts and emits part of its contents. The number of glucose molecules inside the vesicle (N_g) is a function of time, as the difference of glucose concentration inside and outside the vesicle initiates the flow of glucose molecules into the vesicle through the EqT-II induced pores in the membrane. The flux of the glucose molecules at a given concentration difference ($\Delta C = C_{go} - C_g$) outside and inside the vesicle is:

$$j = P\Delta C, \tag{5}$$

in which P is the permeability of the membrane. The number of glucose molecules increases as:

$$\frac{dN_g}{dt} = PA\left(C_{go} - \frac{N_g}{V}\right). \tag{6}$$

When solving Eq. 6, it has to be considered that the volume of the vesicle V is not constant, but dependent on the number of glucose molecules inside the vesicle. As the permeability of the membrane depends on the density of the pores in the membrane and the permeability of the individual pore does not change during the vesicle growth, the product PA remains constant.

The dependence of the vesicle volume on the number of the glucose molecules inside the vesicle can be obtained by equating Eqs. 3 and 4. After expanding the resulting equation around the starting radius r_0 and linearizing it, the dependence of the small changes of volume (ΔV) on the number of glucose molecules that have entered the vesicle (ΔN_g) can be written in a simple form:

$$\Delta V = \frac{\Delta N_g}{\left(\frac{4k_a}{3kTr_0} + C_{go}\right)}. \tag{7}$$

The number of glucose molecules that diffuse into the vesicle between two bursts ($\Delta N_{g,max}$) is proportional to the maximal volume increase (ΔV_{max}) and is always the same. The number of sucrose molecules $N_{s,i}$ enclosed in the vesicle is changing from burst to burst, but is constant in the time interval between the bursts. According to the model the number of sucrose molecules emitted in the jet during the ith burst ($\Delta N_{s,i}$) is proportional to the number of sucrose molecules inside the vesicle just before the ith burst ($N_{s,i}$):

$$\Delta N_{s,i} = \frac{\Delta V_{max}}{V_{max}} N_{s,i} \tag{8}$$

and thus decreases exponentially as a function of the number of bursts. The factor of proportionality is the ratio of the volume that is ejected during each burst (ΔV_{max}) and the maximum volume reached just before the burst (V_{max}). With the number of sucrose molecules inside the vesicle determined immediately after two successive bursts the ratio of volumes can be calculated and the allowed change of radius (Δr_{max}) determined.

Eq. 6 was expanded around the starting vesicle volume V_0 and linearized for small changes of the volume between the successive bursts. The time interval between two successive bursts (t_i) can then be expressed as:

$$t_i = -\frac{t_0}{b}\ln\left(1 - \frac{b\Delta N_{g,max}}{N_{s,i}}\right), \tag{9}$$

$$t_0 = \frac{V_0}{PA},$$

$$b = \frac{\frac{4k_a}{3kTr_0} + \frac{N_{s,i}}{V_0}}{\frac{4k_a}{3kTr_0} + C_{go}}.$$

Eq. 9 was solved step by step. The initial conditions are known and the number of sucrose molecules inside the vesicle can be calculated through the known concentration of sucrose solution and the known vesicle volume. Then the number of glucose molecules inside the vesicle just before the burst was obtained from Eq. 7 and the time of the burst determined from Eq. 9. From the calculated numbers of glucose and sucrose molecules emitted during the burst (from Eq. 8) the numbers of glucose and sucrose molecules that remained inside the vesicle were determined. The initial conditions for the next step of solving the Eq. 9 were thus determined. This way we were able to predict the increasing of the glucose fraction and decreasing of the sucrose fraction in the vesicle as a function of time, the changing of the radius with time, and the increasing of time intervals between the bursts.

Results of the analysis

For carrying out the calculations, presented by Eqs. 7 and 9, we needed to obtain an estimate of the change of radius that is allowed by the elastic properties of the membrane. As Eq. 8 implies, the proportionality factor $\Delta V_{max}/V_{max}$ can be calculated from the data on the sucrose concentration immediately after two successive bursts. The value of the critical radius to which the membrane strains can therefore be obtained indirectly through the measurements of the sucrose fraction at the moment of the bursts. We obtained the change of the vesicle radius to be $\Delta r_{max} = (0.02 \pm 0.002)r_0$ (from six measurements) (Fig. 9 *B*). This is in agreement with the data on the vesicle average maximum area expansion (Bloom et al., 1991). Also the direct measurements of the diameter changes agree with these results (not shown). However, the direct measurements are less reliable because the vesicle membrane is hidden inside the halo and its position cannot be accurately determined.

For each concentration of toxin in the glucose solution, we adjusted the model predictions to the data obtained by the measurements, and determined the permeability of the membrane. An example of this procedure is illustrated in Fig. 8, *A* through *D*. In each figure the time course of change of the sucrose fraction in the vesicle is shown for three of the analyzed vesicles. Full lines represent the results of the model, where the average permeability of all analyzed vesicles was used. In Table 1 the values of the membrane permeability, obtained by the comparison of the measurements and the model, are given.

The dependence of membrane permeability on toxin concentration is illustrated in Fig. 10 *A*. By introducing a

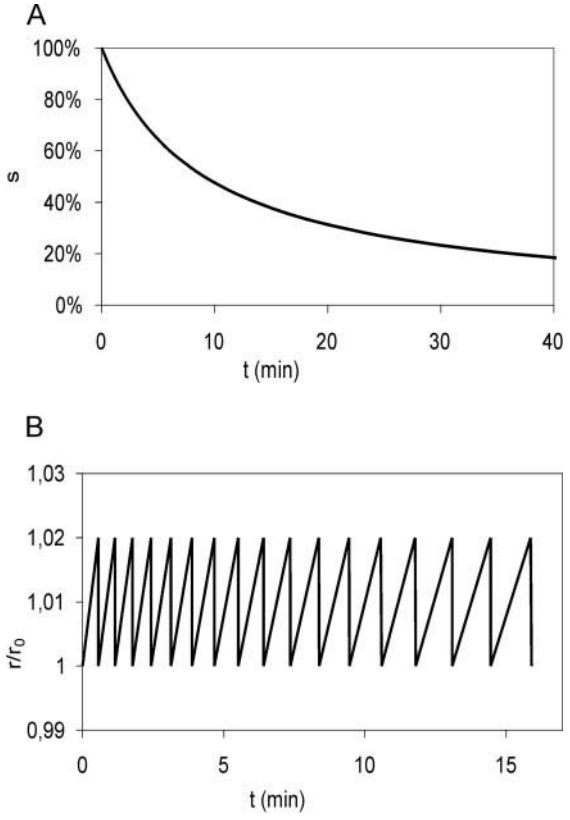

FIGURE 9 (*A*) Time dependence of the sucrose fraction (*s*, in percentage) in the vesicle and (*B*) the time dependence of the vesicle radius (r/r_0, $r_0 = 50\ \mu m$) with membrane permeability $P = 3.2 \times 10^{-6}$ cm/s as predicted by the theoretical model.

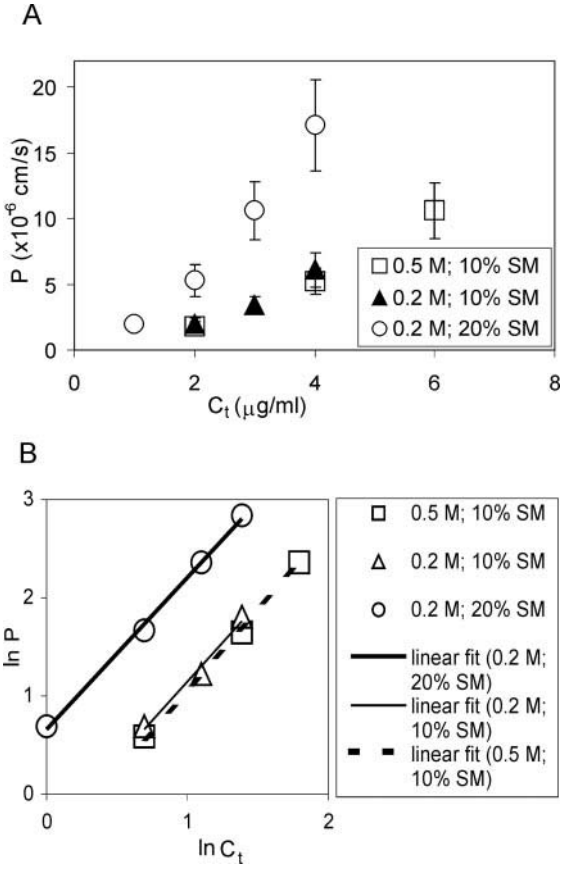

FIGURE 10 (*A*) Membrane permeability (*P*) for the molecules of glucose as a function of the toxin EqT-II concentration (C_t). (*B*) Dependence of membrane permeability (*P*) on toxin EqT-II concentration (C_t), plotted in double logarithmic scale. The slope of the line (the Hill number) is 1.6 ± 0.7.

double-logarithmic plot of the permeability of the membranes versus toxin concentration (Fig. 10 *B*), we determined the Hill number as the slope of the plotted curves, $nH = 1.6 \pm 0.7$, indicating the cooperation of the toxin monomers in the pore formation. The permeability of the membrane is proportional to the density of pores in the membrane, whereas the number of toxin molecules (*N*), embedded in the membrane, is proportional to the toxin concentration in the glucose solution (C_t), hence $N = aC_t$. The coefficient *a* describes the affinity of the membrane to bind the EqT-II molecules. In logarithmic mode ($\text{Ln}\ C_t = \text{Ln}\ N - \text{Ln}\ a$) this implies the shifting of the curve to the left, when the curve describes the permeability of the membranes with greater affinity to bind toxin molecules (the membranes with greater SM fraction).

TABLE 1 Average permeability of the membranes for glucose molecules at different molarities of sugar solutions, different vesicle membrane compositions, and different concentrations of equinatoxin II

Sugar solution	Membrane composition	EqT-II concentration (μg/mL)	Membrane permeability ($\times 10^{-6}$ cm/s)
0.5 M	0.9 POPC and 0.1 SM	2	1.8 ± 0.4
0.5 M	0.9 POPC and 0.1 SM	4	5.2 ± 1.0
0.5 M	0.9 POPC and 0.1 SM	6	10.6 ± 2.1
0.2 M	0.9 POPC and 0.1 SM	2	2.0 ± 0.4
0.2 M	0.9 POPC and 0.1 SM	3	3.4 ± 0.7
0.2 M	0.9 POPC and 0.1 SM	4	6.1 ± 1.3
0.2 M	0.8 POPC and 0.2 SM	1	2.0 ± 0.5
0.2 M	0.8 POPC and 0.2 SM	2	5.3 ± 1.2
0.2 M	0.8 POPC and 0.2 SM	3	10.6 ± 2.2
0.2 M	0.8 POPC and 0.2 SM	4	17.1 ± 3.5

DISCUSSION

The methodology described enabled the study of the membrane transport by observing optically the behavior of the giant vesicles. The mechanism of release of the vesicle contents was revealed and explained. The dynamics of the changing of the composition of the vesicle contents predicted by the analysis is in good agreement with the measured data.

The model was based on a few assumptions, some of which should be commented on and discussed. One of the

basic assumptions, implied by the data from the references and the control experiments was that the water passes through the membrane much faster than the sugars. The permeability for water would probably increase when the membrane is stretched in the phase of vesicle growing and when the contribution of the transport of water through the EqT-II-induced pores is taken into account. All such considerations are irrelevant when an "infinite" water permeability is assumed. The obtained results are therefore the lower limit for the estimates of membrane permeability for glucose.

The induced water flux into the vesicle causes the membrane to stretch and finally burst. A similar opening of the stretched vesicle membrane was observed, and the dynamics of the transient openings analyzed for vesicles in a viscous solvent (Sandre et al., 1999). In our experiment the process of growth and closure of the opening is much faster (Fig. 5), as can be expected because of the lower viscosity of the surrounding solution. In our model the duration of the burst is therefore neglected compared with the time between the bursts.

We compared the measurements and the theoretical predictions only from the first burst on, as we simplified our model by the assumption that the EqT-II molecules embed into the membrane before the first breaking of the membrane and that after the first burst the number of pores is constant. This assumption can be justified by a simple consideration: if the number of pores increased significantly between two successive bursts, the permeability of the membrane would increase and the sucrose fraction inside the vesicle would decrease more rapidly, whereas in our experiment we observed that the time between the consecutive bursts increases. On average the number of pores must therefore be constant throughout the process, and although the properties of the pores may be more complicated and we cannot say anything about the dynamics or the life-time of a pore, the estimated (average) membrane permeability and the predictions of the change of the sucrose fraction inside the vesicle by the simplified model fit the experimental data (Fig. 8).

To test the adequacy of the explanations of the transmembrane solute transport and the reliability of the methods used, our work was compared with the results of the previous studies. The theoretical analysis provided us with the necessary tools for determining the permeability of the membranes at given concentrations of the toxin EqT-II. The results of our analysis of the membrane permeabilization with EqT-II can be related to the results, obtained by Tejuca et al. (1996) by using toxin sticholysin I from the sea anemone *Stichodactyla helianthus*. Sticholysin I is also a potent toxin, in its effects on the cells very similar to the action of EqT-II. SM works as a low-affinity receptor for sticholysin I, which is supposed to form pores of functional radius of around 1 nm in the membranes of the vesicles. The permeabilization was determined by measuring the fluorescence of calcein, released from the vesicles. The authors report fits in double logarithmic plots of the permeability of the membranes versus toxin concentration with Hill numbers from 2.1 ± 0.6 (with 75% of SM in the membrane) to 2.6 ± 0.4 (25% of SM in the membrane).

By monitoring single vesicles under the influence of EqT-II we were able to observe phenomena like growing of the vesicle, bursting of the membrane, and shrinkage of the freshly prepared vesicles that were not previously described. The method of micropipetting enabled us to manipulate single vesicles. We used the otherwise unwelcome optical effect of phase-microscopy (the halo around the vesicles) to obtain information about the changing composition of the vesicle contents. Thus, we were able to study the mechanisms of the sugar transport across the vesicle membrane. Many accompanying problems like diminishing of the vesicle size and formation of the protuberances in freshly prepared vesicles (Fig. 7 *B*) remain open.

We want to thank Ms. Vesna Arrigler for all the help in the laboratory and the preparations of the phospholipid vesicles. We also thank Prof. Dr. Peter Maček for providing us with freshly isolated EqT-II and the information and advice on the toxin action and characteristics.

REFERENCES

Angelova, M. I., S. Soléau, P. Méléard, J. F. Faucon, and P. Bothorel. 1992. Preparation of giant vesicles by external AC electric fields: kinetics and applications. *Progr. Colloid Polym. Sci.* 89:127–131.

Athanasiadis, A., G. Anderluh, P. Maček, and D. Turk. 2001. Crystal structure of the soluble form of equinatoxin II, a pore-forming toxin from the sea anemone *Actinia Equina. Struct.* 9:341–346.

Avila, A. D., M. C. de Acosta, and A. Lage. 1989. A carcioembryonic antigen-directed immunotoxin built by linking monoclonal-antibody to a hemolytic toxin. *Int. J. Cancer.* 43:926–929.

Batista, U., P. Maček, and B. Sedmak. 1990. The cytotoxic and cytolytic activity of equinatoxin II from sea anemone *Actinia equina. Cell Biol. Int. Rep.* 14:1013–1024.

Belmonte, G., G. Menestrina, C. Pederzolli, I. Križaj, F. Gubenssek, T. Turk, and P. Maček. 1994. Primary and secondary structure of a pore-forming toxin from the sea anemone, *Actinia equina L.*, and its association with lipid vesicles. *Biochim. Biophys. Acta.* 1192:197–204.

Belmonte, G., C. Pederzolli, P. Maček, and G. Menestrina. 1993. Pore formation by the sea anemone cytolysin equinatoxin II in red blood cells and model lipid membranes. *J. Membr. Biol.* 131:11–22.

Bhakdi, S., U. Weller, I. Walev, E. Martin, D. Jonas, and M. Palmer. 1993. A guide to the use of pore-forming toxins for controlled permeabilization of cell-membranes. *Med. Microbiol. Immunol.* 182:167–175.

Bloom, M., E. Evans, and O. G. Mouritsen. 1991. Physical properties of the fluid - bilayer component of cell membranes: a perspective. *Q. Rev. Biophys.* 24:293–397.

Caaveiro, J. M. M., I. Echabe, I. Gutiérrez-Aguirre, J. L. Nieva, J. L. R. Arrondo, and J. M. Gonzáles-Mañas. 2001. Differential interaction of equinatoxin II with model membranes in response to lipid composition. *Biophys. J.* 80:1343–1353.

De Los Rios, V., J. M. Mancheño, M. E. Lanio, M. Oñaderra, and J. G. Gavilanes. 1998. Mechanism of the leakage induced on lipid model membranes by the hemolytic protein sticholysin II from the sea anemone *Stichodactyla helianthus. Eur. J. Biochem.* 252:284–289.

Ho, C. L., J. L. Ko, H. M. Lue, C. Y. Lee, and I. Ferlan. 1987. Effect of equinatoxin on the guinea-pig atrium. *Toxicon.* 25:659–664.

Jung, C. Y. 1971. Permeability of bimolecular membranes made from lipid extracts of human red cell ghosts to sugars. *J. Membr. Biol.* 5:200–214.

Lee, C. Y. 1989. Cardiovascular effects of equinatoxin, a basic protein from the sea anemone *Actinia equina. In* Biosignalling in Cardiac and Vascular Systems. M. Fujiwara, S. Narumiya, and S. Miwa, editors. Pergamon, Oxford. 380–384.

Maček, P., G. Belmonte, C. Pederzolli, and G. Menestrina. 1994. Mechanism of action of equinatoxin II, a cytolysin from the sea anemone *Actinia equina L.* belonging to the family of actinoporins. *Toxicology.* 87:205–227.

Maček, P., and D. Lebez. 1981. Kinetics of hemolysis induced by equinatoxin, a cytolytic toxin from the sea anemone *Actinia equina*: effect of some ions and pH. *Toxicon*. 19:233–240.

Maček, P., M. Zecchini, C. Pederzolli, M. Dalla Serra, and G. Menestrina. 1995. Intrinsic tryptophan fluorescence of equinatoxin II, a pore forming polypeptide from sea anemone *Actinia equina L.*, monitors its interaction with lipid membranes. *Eur. J. Biochem.* 234:329–335.

Olbrich, K., W. Rawicz, D. Needham, and E. Evans. 2000. Water permeability and mechanical strength of polyunsaturated lipid bilayers. *Biophys. J.* 79:321–327.

Pluta, M. 1989. Advanced Light Microscopy, Vol. 2. Elsevier, Amsterdam.

Russo, M. J., H. Bayley, and M. Toner. 1997. Reversible permeabilization of plasma membranes with an engineered switchable pore. *Nat. Biotechnol.* 15:278–282.

Sandre, O., L. Moreaux, and F. Brochard-Wyart. 1999. Dynamics of transient pores in stretched vesicles. *Proc. Natl. Acad. Sci. U.S.A.* 96:10591–10596.

Tejuca, M., M. Dalla Serra, M. Ferreras, M. E. Lanio, and G. Menestrina. 1996. Mechanism of membrane permeabilisation by sticholysin I, a cytolysin isolated from the venom of the sea anemone *Stichodactyla helianthus. Biochemistry.* 35:14947–14957.

Valcarel, C. A., M. Dalla Serra, C. Potrich, I. Bernhart, M. Tejuca, D. Martinez, F. Pazos, M. E. Lanio, and G. Menestrina. 2001. Effects of lipid composition on membrane permeabilization by sticholysin I and II, two cytolysins of the sea anemone *Stichodactyla helianthus. Biophys. J.* 80:2761–2774.

Zorec, R., M. Tester, P. Maček, and W. T. Mason. 1990. Cytotoxicity of equinatoxin II from the sea anemone *Actinia equina* involves ion channel formation and an increase in intracellular calcium activity. *J. Membr. Biol.* 118:243–249.